Direct observation of a roaming intermediate and its dynamics

Grite L. Abma,[1] Michael A. Parkes,[2] Weronika O. Razmus,[3]
Yu Zhang,[4] Adam S. Wyatt,[4] Emma Springate,[4] Richard T. Chapman,[4]
Daniel A. Horke,[1*], Russell S. Minns[3*]
[1]Radboud University, Institute for Molecules and Materials,
Heijendaalseweg 135, 6525 AJ Nijmegen, The Netherlands
[2]Department of Chemistry, University College London, 20 Gordon Street, London
[3]School of Chemistry, University of Southampton,
Highfield, Southampton SO17 1BJ, UK
[4]Central Laser Facility, STFC Rutherford Appleton Laboratory,
Didcot, Oxfordshire OX11 0QX, UK
*To whom correspondence should be addressed;
DAH: d.horke@science.ru.nl, RSM: r.s.minns@soton.ac.uk.

(Dated: March 31, 2023)

Abstract

Chemical reactions are often characterised by their transition state, which defines the critical geometry the molecule must pass through to move from reactants to products. Roaming provides an alternative picture, where in a dissociation reaction the bond breaking is frustrated, and a loosely bound intermediate is formed. Following bond breaking the two partners are seen to roam around each other at distances of several Angstroms, forming a loosely bound, and structurally ill-defined, intermediate that can subsequently lead to reactive or unreactive collisions. Here we present a direct and time-resolved experimental observation of roaming. By measuring the photoelectron spectrum of UV excited acetaldehyde with a femtosecond extreme ultraviolet pulse, we captured spectral signatures of all of the key reactive structures including that of the roaming intermediate. This provided a direct experimental measurement of the roaming process and allowed us to identify the timescales by which the roaming intermediate is formed and removed, and the electronic potentials upon which roaming proceeds.

The traditional view of a chemical reaction relies on transition state theory, where specific structures act as bottlenecks through which reactants must pass to form products. Over the course of the past 15 years a new type of photodissociation reaction mechanism, termed 'roaming', has challenged this view and is thought to compete with transition state driven dynamics.[1–6] This roaming pathway can occur when, on route to dissociation, a shallow plateau in the potential energy surface is encountered, leading to the formation of a quasi-bound complex of two fragments. This quasi-bound roaming intermediate then explores a broad range of structures around a weakly-bound plateau region of the potential energy surface, before reaching a point in configuration space where the two fragments either react or dissociate completely.

Roaming was first discovered in formaldehyde, where an intermediate is formed by a hydrogen atom roaming around a CHO radical.[1] Since this first observation the roaming pathway has been experimentally shown in a number of systems and is thought to be nearly ubiquitous in photodissociation reactions.[4,7,8] Direct experimental observation of the roaming intermediates is however challenging, meaning that roaming processes have largely been identified through the detailed analysis of the energy partitioning observed in the final reaction products and usually a bimodal internal energy distribution of the fragments has been used as evidence of roaming processes.[2,3,9]

The challenge to experiment is that the characteristics of roaming intermediates place extreme constraints on the measurement processes used. By its very nature, the occurrence of roaming produces a molecular complex that has an ill-defined geometry as the reaction intermediate. The roaming partners can take on a wide range of structures defined by a broad plateau on the potential energy surface. The typically rapid formation of the intermediate and subsequent slow decay necessitates measurements on timescales covering many orders of magnitude, potentially from femtoseconds to nanoseconds. These characteristics provide a demanding backdrop to experiment and theory alike. Accurate theoretical descriptions of the roaming wavepacket are difficult to perform, while the identification of specific structural or spectral probes are challenging to experiments.

Experimental probes that are sensitive to all aspects of the roaming dynamics are needed, ideally capturing the formation and decay of the roaming intermediate, as well as the final products formed. To the best of our knowledge, the only experimental observation of a roaming intermediate was only recently reported. Utilising a time-resolved Coulomb explosion

imaging measurement with coincident detection of multiple fragment ions, the authors were able to identify a signature of the first step in the roaming process in formaldehyde, as well as the formation of the intermediate complex on a timescale of a few hundred femtoseconds.[6] However, a full time-resolved measurement of roaming dynamics, and of the eventual fate of the intermediate, has so far not been reported.

Herein we report on the direct and time-resolved observation of the formation and subsequent decay of the roaming intermediate in the photodissociation of acetaldehyde (CH_3CHO). Here UV absorption leads to the carbon-carbon bond breaking and the formation of CH_3 and HCO radicals. The radicals begin to separate and can either follow a pathway that is well described by transition state theory and rapidly leads to the separation of the two radical fragments, or a roaming pathway where the two fragments are seen to remain in relative close proximity (at C−C distances of 3-4 Å[4]) for an extended period of time. For the molecules that follow the roaming pathway, the two radicals explore a wide range of configurations before reaching one that allows for reaction of the two fragments, forming CH_4 and CO, or dissociation leading to the delayed formation of the radical products. The roaming channel in this photodissociation has been studied by various groups both theoretically[10–12] and experimentally[3,9,13–19] and at a vast range of dissociation energies from ∼220–330 nm.[17] The primary experimental observable in all these studies was the energy distribution of final radical (HCO, CH_3) or molecular (CO, CH_4) products, meaning a direct observation of the roaming intermediate, and its formation pathway, has so far remained elusive. Existing time-resolved studies lack the necessary temporal resolution to observe the crucial first electronic dynamics following photoexcitation.[14,15] Here we study the ultrafast dynamics following excitation of acetaldehyde at 262 nm (4.7 eV), populating the first electronically excited state (S_1) via a $\pi^* \leftarrow n$ transition.[20] At this excitation energy the dissociation mechanism is not well understood, with some studies invoking intersystem crossing to lower lying triplet states as a potential relaxation pathways,[14,19] while others suggest that at these pump wavelengths the available energy is sufficient to surpass a barrier on the S_1 surface, leading to internal conversion via a conical intersection with the singlet ground state S_0.[10,11,16–18] Following internal conversion the system can either directly dissociate, or it can lead to roaming by exploring a wide plateau on the potential surface, eventually leading to both radical and molecular dissociation channels. To directly observe the formation and subsequent destruction of the roaming intermediate, we present here a photoelectron

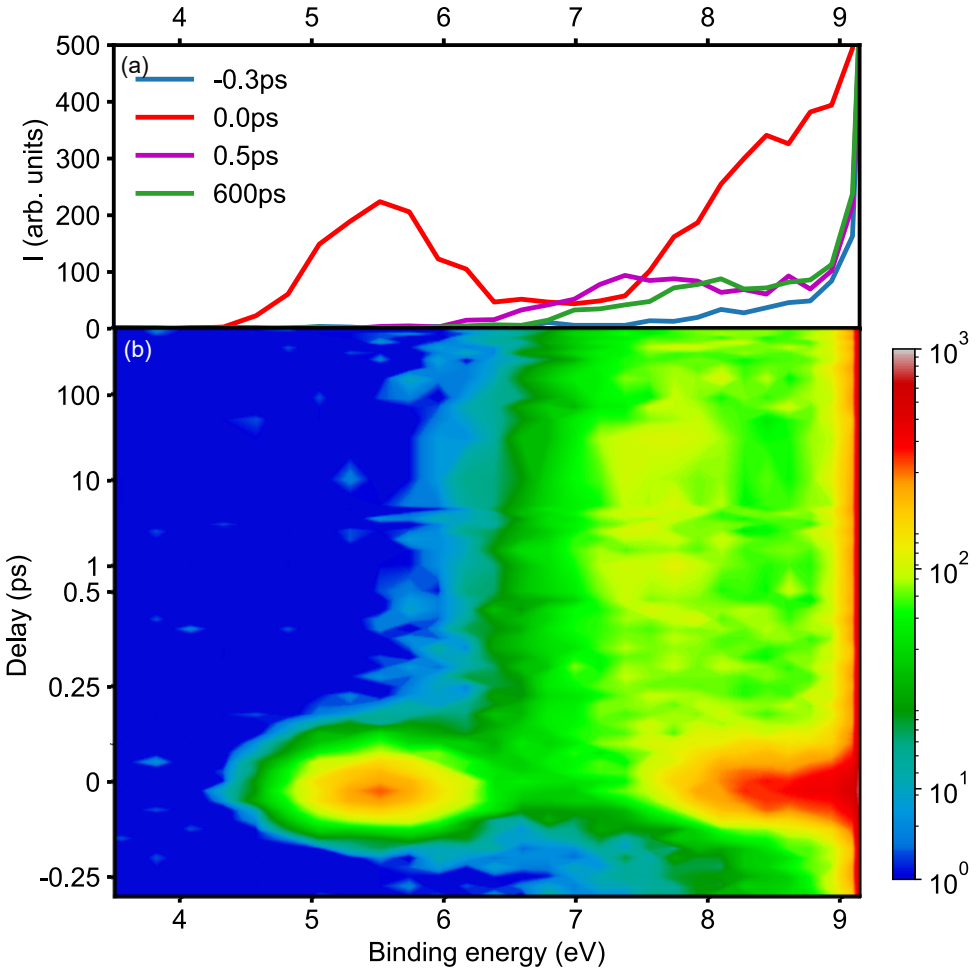

FIG. 1. Time-resolved photoelectron spectra of acetaldehyde following excitation at 262 nm and ionisation at 56 nm (22.3 eV). a) Selected spectra at different pump-probe delays, before t_0(blue), at t_0(red), at 500 fs (purple) and at long delays of 600 ps (green). b) Surface plot showing the time evolution of the photoelectron spectra, note the mixed linear-logarithmic time delay (y) axis.

spectroscopy experiment utilizing a femtosecond extreme ultraviolet (XUV) probe pulse.[21] The sensitivity of photoelectron spectroscopy to changes in the bonding character, combined with the high energy of the probe, allowed us to monitor all aspects of a roaming reaction.[22,23] The measurements captured spectroscopic signatures of the formation and removal of roaming intermediates, as well as the formation of the CHO radical product via direct and roaming reaction pathways. The experimental data is supported by *ab-initio* calculations of the potential energy surfaces and simulated photoelectron spectra, which allowed us to identify the electronic state upon which roaming proceeds.

Resulting photoelectron spectra are shown in Figure 1. In panel **a** we show characteristic photoelectron spectra at selected pump-probe delays. With pump and probe pulses temporally overlapped (t_0, red trace) we observe two broad peaks centred around binding energies of 5.5 eV and 8.5 eV. These correspond to ionisation of the initially excited state of the bound CH_3CHO molecule into the ground (D_0) and first electronically excited (D_1) state of the ion, respectively. These features are very short lived, and by 500 fs (purple trace) we observe only a very broad feature from around 6.0 eV to at least 9.0 eV of binding energy, beyond this energy any signals are obscured by the direct ionisation of ground state acetaldehyde, as further discussed in the supplementary information. Going towards even longer delays (600 ps, green trace) this broad feature has narrowed and shifted towards higher binding energies, and now corresponds to final reaction products, in this case the formation of the HCO radical, as further discussed below.

In Figure 1**b** we show the full time-resolved photoelectron spectrum, note the mixed linear-logarithmic scale on the time delay (y) axis. The full spectrum highlights the very short lived nature of the initially excited state, and the formation of a broad peak within a few hundred femtoseconds. On longer timescales of hundreds of picoseconds this peak is seen to decrease in intensity on the low binding energy side.

To extract dynamic information we integrate the time-resolved spectrum over selected binding energy slices, Figure 2. The green trace in panel **a** shows the dynamics in the 5.2–5.8 eV binding energy region, corresponding to the initially excited state in acetaldehyde. A rapid exponential decay with a time constant of around 50 fs is observed, which we assign to the rapid depopulation of the initially excited S_1 state. The blue traces in Figure 2**a**–**b** show the binding energy region of 6.7–7.3 eV. Following a fast rise, a slow decay on a timescale of a few hundred picoseconds is observed, until a plateau of around half the intensity is reached. This behaviour clearly indicates multiple overlapping contributions to the photoelectron spectrum, belonging to a transient state decaying on the 100s of picosecond timescale, and a (much) longer lived contribution likely from a reaction product. In order to deconvolve these we perform a global 2D fit to the entire time-resolved photoelectron spectrum to extract so-called decay-associated spectra (DAS), which represent the spectral contribution to each underlying dynamical process. We require a total of 3 separate processes, each with its own associated lifetime, to accurately represent the data.

The resultant DAS are plotted in Figure 3, and have associated time constants of 50 fs,

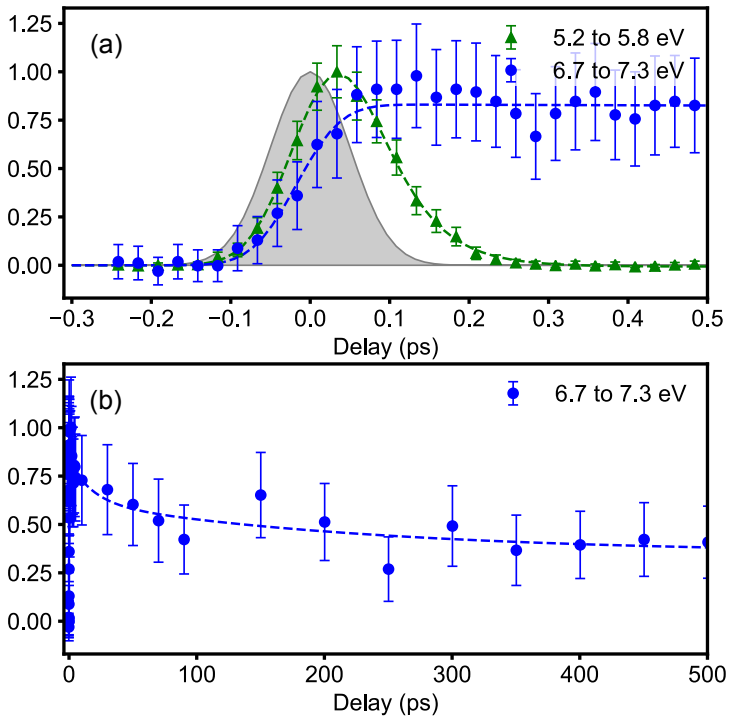

FIG. 2. Time evolution of the observed photoelectron signal in selected energy regions on short (a) and long (b) timescales. Grey shading in (a) corresponds to the instrument response function.

>3 ns and 170 ps in panels **a**–**c**, respectively. At early times the dynamics are dominated by the spectral contribution shown in the top panel of Figure 3. The broad peaks correlate well with the expected binding energies for ionisation from the Franck-Condon geometry of the initially excited S_1 state. These peaks have an associated time constant of approximately 50 fs, meaning this is an extremely short lived configuration of the molecule.

In Figure 3**b** we show the spectral component that has an associated lifetime of >3 ns. This is much longer than the timescale of our experiment and hence can be considered an 'infinite lifetime', such that on the timescale covered here the intensity remains unchanged and this corresponds to a product state of the reaction. Based on the known reaction products and their ionisation energies, (CH_3 9.84 eV , CHO 8.1 eV, CH_4 12.61 eV, CO 14.01 eV)[24] we assign this feature to the rapid formation of CHO, occurring within the first 100 fs after excitation.

The lower panel in Figure 3 shows a more complex spectrum, including regions of positive and negative amplitude, with an associated time constant of 170 ps. In DAS regions of positive amplitude relate to spectral features that decay on the associated timescale (as

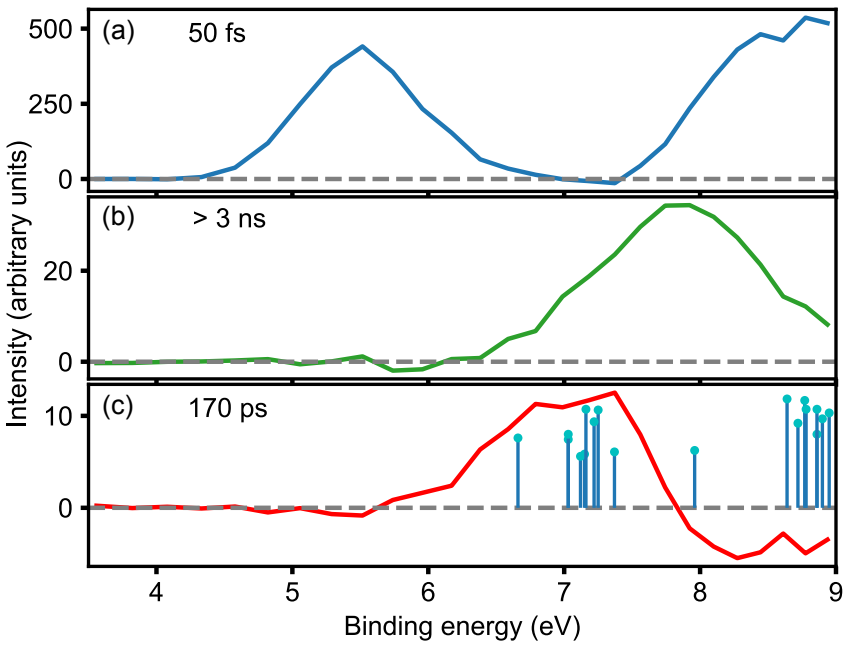

FIG. 3. Decay associated spectra extracted from the experimental data in Figure 1. Three time constants of 50 fs (a), >3 ns (b) and 170 ps (c) are required to accurately represent the data. In panel (c) calculated binding energies following ionisation of the roaming intermediate in various geometries on the S_0 state are indicated as sticks, with the length corresponding to the relative cross-section.

seen in Figure 3**a**–**b**), whilst negative amplitudes relate to spectral features that increase in intensity on that timescale. The observation of both positive and negative amplitudes within the DAS is therefore a direct sign for the flow of population from one region of the spectrum, where positive amplitude is observed, to regions of the spectrum with a negative amplitude. Figure 3**c** therefore clearly shows the decay of a species with binding energies in the range 5.3–7.6 eV into a new species with higher binding energies on a timescale of 170 ps. At these higher binding energies the signal strongly overlaps with the observed CHO peak (Figure 3**b**), indicating that we are producing further CHO fragments over this much longer time scale, in addition to those produced from the rapid initial dissociation. The observed feature in the 5.3–7.6 eV range therefore corresponds to a reactive intermediate, formed within the first few hundred femtosecond after excitation, and decaying on a 170 ps timescale to yield (as one product) the CHO radical. We therefore assign this transient species to the roaming intermediate $CH_3 \cdots CHO$. The observed binding energy is indicative

of an intermediate structure between a bound CH_3CHO and the radical product CHO, suggesting we are monitoring a range of structures associated with the weakly bound roaming intermediate. The observed rapid appearance of the intermediate within the first few hundred femtoseconds agrees well with recent observations in formaldehyde.[6]

In order to support our assignments, and to understand where on the potential energy surface roaming takes place, we calculated the coupled potential energy surfaces important to the dynamics, technical details are given in the supporting information. The acetaldehyde potential energy surface was explored at a range of C−C bond lengths and C−C−H bond angles. A projection of the initially excited S_1 and ground state S_0 surfaces are plotted in Figure 4**a**, with panel **b** showing a contour projection of the S_1 surface. The figure shows an extended crossing (points of degeneracy) between the two surface at a C−C−H angle of 50° with C−C bond lengths of greater than 2.5 Å(indicated by the dashed line in Figure 4**b**). Efficient population transfer is facilitated at these crossing points (conical intersection seam) allowing for rapid re-population of the electronic ground state. Surrounding this crossing associated with the conical intersection is a broad and flat plateau extending over a wide range of angles and bond lengths. We note that within the figure we can only provide a limited projection of the full potential energy surface (which would contain 15 dimensions) and this plateau extends over a much wider range of geometries than can be plotted within a single projection.

The ground and excited state potential energy surfaces then provide us with a landscape upon which we can calculate theoretical photoelectron spectra for a variety of geometries associated with the initially excited Franck-Condon geometry, the dissociated fragments and the roaming intermediate. Full details on the calculations can be found in the SI as we limit the presentation here to the calculated photoelectron energies for ionisation of the roaming intermediate on the ground electronic state. Calculated energies and relative cross-sections for various geometries on the broad plateau region are shown in Figure 3**c**, overlayed with the experimental photoelectron spectrum assigned to the roaming intermediate. The calculations show a broad range of binding energies are possible, correlating with the 'floppy' structure of the molecule and the large areas of the potential energy surface explored. Importantly, a number of calculated photoelectron energies agree remarkably well with the feature assigned to the roaming intermediate, in the range of ∼6–8 eV binding energy, giving us confidence in the assignment of this feature to the roaming intermediate. A further cluster of expected

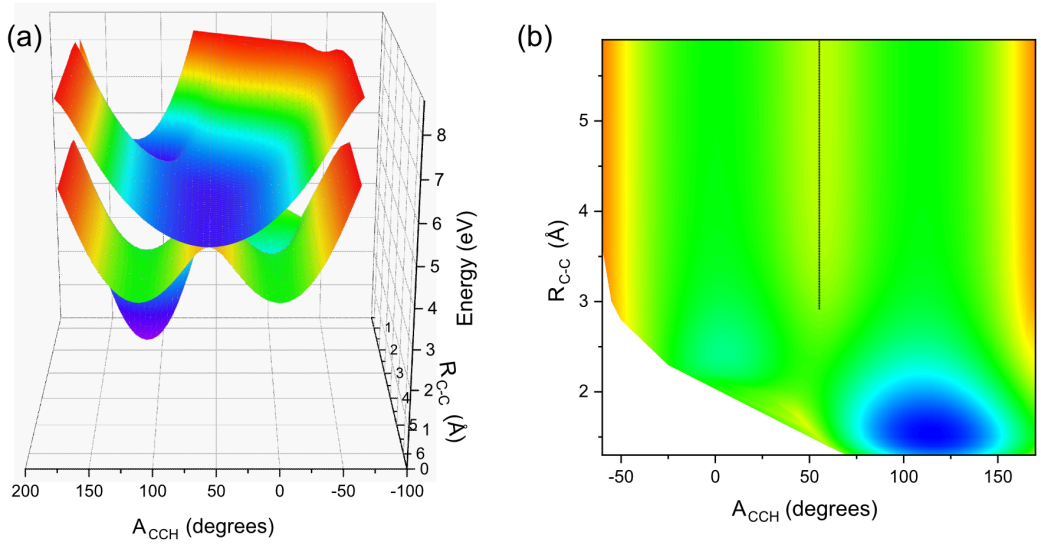

FIG. 4. Calculated potential energy surfaces of acetaldehyde. (a) Projection of the S_1 and S_0 surfaces along the C-C bond length and CCH bond angle coordinates. (b) Contour plot of the S_0 ground state surface, the dashed line indicated a conical intersection seam with the S_1 state.

photoelectron peaks is towards higher binding energies of > 8 eV. Experimentally, this signal on the high binding energy side is, however, obscured by the contributions from the CHO radical, and beyond ~ 9 eV from the ground state ionisation of acetaldehyde.

The combined experimental and theoretical results lead to the following picture of the dynamics. Absorption of a UV photon leads to population of the S_1 excited state. Here, the C−C bond distance increases on route to a conical intersection, where there is efficient population transfer *via* a conical intersection to the S_0 ground state,[10,16–18] the extremely fast timescale rules out any intersystem crossing into the triplet state. Once in the ground state a subset of the initially excited molecules continues along the dissociation path leading to the rapid (50 fs) formation of the CH_3 and HCO fragments. The remaining quasi-bound population is associated with roaming dynamics of the CH_3 and HCO fragments, which explore a range of structures on the ground state potential. This roaming intermediate decays with a time constant of 170 ps and we observe the concomitant formation of further isolated HCO fragments on this timescale. We note that the formation of other products, such as CH_4+CO or reformation of a vibrationally hot ground state molecule, will also contribute to the effective lifetime measured.

The sensitivity of our XUV photoelectron spectroscopy probe allowed us to monitor the

key geometric and electronic structure changes associated with roaming dynamics for the first time. We directly observed the formation of the roaming intermediate on an ultrafast (<100 fs) timescale. Detailed analysis of the resulting photoelectron spectrum and comparison to quantum chemical calculations allow us to identify that roaming occurs on the electronic ground state, and that the eventual breakdown of the roaming intermediate occurs on a 170 picoseconds timescale. These experiments employing global probes with ultrafast time-resolution offer the chance for a detailed and direct insight into molecular roaming pathways, and to quantify the importance and prevalence of roaming processes in photochemistry.

Acknowledgments

The authors thank the STFC for access to the Artemis facility. RSM acknowledges the EPSRC (EP/R010609/1) for research support. WOR thanks the UK Hub for the Physical Sciences on XFELS (STFC) and the University of Southampton for a studentship. DAH and GLA acknowledge support by the Netherlands Organization for Scientific Research (NWO) under grant numbers 712.018.004 and VI-VIDI-193.037, and would furthermore like to thank the Spectroscopy of Cold Molecules Department, and in particular Prof. Bas van de Meerakker, for the continued support. We also thank Phil Rice and Alistair Cox for technical assistance. For the purpose of open access, the author has applied a Creative Commons Attribution (CC BY) licence to any Author Accepted Manuscript version arising.

Author Contributions

The experiment was conceived by RSM with input on the planning and implementation from DAH and RTC. GLA, WOR, MAP and RSM collected the data with support from RTC, YZ, ASW and ES who run and manage the Artemis laser facility. The experimental data was analysed by GLA and DAH and the theoretical calculations performed by MAP. The combined output from the experiment and calculations were interpreted by GLA, MAP, WOR, RTC, DAH and RSM. The manuscript was written by RSM, GLA and DAH with input and edits from all authors.

References

[1] Townsend, D.; Lahankar, S. A.; Lee, S. K.; Chambreau, S. D.; Suits, A. G.; Zhang, X.; Rheinecker, J.; Harding, L. B.; Bowman, J. M. The Roaming Atom: Straying from the Reaction Path in Formaldehyde Decomposition. *Science* **2004**, *306*, 1158–1161.

[2] Grubb, M. P.; Warter, M. L.; Xiao, H.; Maeda, S.; Morokuma, K.; North, S. W. No Straight Path: Roaming in Both Ground- and Excited-State Photolytic Channels of $NO_3 \rightarrow NO + O_2$. *Science* **2012**, *335*, 1075–1078.

[3] Heazlewood, B. R.; Jordan, M. J. T.; Kable, S. H.; Selby, T. M.; Osborn, D. L.; Shepler, B. C.; Braams, B. J.; Bowman, J. M. Roaming Is the Dominant Mechanism for Molecular Products in Acetaldehyde Photodissociation. *Proc. Natl. Acad. Sci. U.S.A.* **2008**, *105*, 12719–12724.

[4] Suits, A. G. Roaming Reactions and Dynamics in the van Der Waals Region. *Annu. Rev. Phys. Chem.* **2020**, *71*, 77–100.

[5] Quinn, M. S.; Nauta, K.; Jordan, M. J. T.; Bowman, J. M.; Houston, P. L.; Kable, S. H. Rotational Resonances in the H_2CO Roaming Reaction Are Revealed by Detailed Correlations. *Science* **2020**, *369*, 1592–1596.

[6] Endo, T. et al. Capturing Roaming Molecular Fragments in Real Time. *Science* **2020**, *370*, 1072–1077.

[7] Bowman, J. M.; Suits, A. G. Roaming Reactions: The Third Way. *Physics Today* **2011**, *64*, 33–37.

[8] Bowman, J. M.; Houston, P. L. Theories and Simulations of Roaming. *Chem. Soc. Rev.* **2017**, *46*, 7615–7624.

[9] Houston, P. L.; Kable, S. H. Photodissociation of Acetaldehyde as a Second Example of the Roaming Mechanism. *Proc. Natl. Acad. Sci. U.S.A.* **2006**, *103*, 16079–16082.

[10] Gherman, B. F.; Friesner, R. A.; Wong, T.-H.; Min, Z.; Bersohn, R. Photodissociation of Acetaldehyde: The CH4+CO Channel. *J. Chem. Phys.* **2001**, *114*, 6128–6133.

[11] Shepler, B. C.; Braams, B. J.; Bowman, J. M. "Roaming" Dynamics in CH_3CHO Photodissociation Revealed on a Global Potential Energy Surface. *J. Phys. Chem. A* **2008**, *112*, 9344–9351.

[12] Harding, L. B.; Georgievskii, Y.; Klippenstein, S. J. Roaming Radical Kinetics in the Decomposition of Acetaldehyde. *J. Phys. Chem. A* **2010**, *114*, 765–777.

[13] Lee, K. L. K.; Quinn, M. S.; Maccarone, A. T.; Nauta, K.; Houston, P. L.; Reid, S. A.; Jordan, M. J. T.; Kable, S. H. Two Roaming Pathways in the Photolysis of CH $_3$ CHO between 328 and 308 Nm. *Chem. Sci.* **2014**, *5*, 4633–4638.

[14] Yang, C.-H.; Bhattacharyya, S.; Liu, L.; Fang, W.-h.; Liu, K. Real-Time Tracking of the Entangled Pathways in the Multichannel Photodissociation of Acetaldehyde. *Chem. Sci.* **2020**, *11*, 6423–6430.

[15] Toulson, B. W.; Kapnas, K. M.; Fishman, D. A.; Murray, C. Competing Pathways in the Near-UV Photochemistry of Acetaldehyde. *Phys. Chem. Chem. Phys.* **2017**, *19*, 14276–14288.

[16] Rubio-Lago, L.; Amaral, G. A.; Arregui, A.; Izquierdo, J. G.; Wang, F.; Zaouris, D.; Kitsopoulos, T. N.; Bañares, L. Slice Imaging of the Photodissociation of Acetaldehyde at 248 Nm. Evidence of a Roaming Mechanism. *Phys. Chem. Chem. Phys.* **2007**, *9*, 6123.

[17] Rubio-Lago, L.; Amaral, G. A.; Arregui, A.; González-Vázquez, J.; Bañares, L. Imaging the Molecular Channel in Acetaldehyde Photodissociation: Roaming and Transition State Mechanisms. *Phys. Chem. Chem. Phys.* **2012**, *14*, 6067.

[18] Heazlewood, B. R.; Rowling, S. J.; Maccarone, A. T.; Jordan, M. J. T.; Kable, S. H. Photochemical Formation of HCO and CH3 on the Ground S0 (A1′) State of CH3CHO. *J. Chem. Phys.* **2009**, *130*, 054310.

[19] Yang, C.-H.; Bhattacharyya, S.; Liu, K. Time-Resolved Pair-Correlated Imaging of the Photodissociation of Acetaldehyde at 267 Nm: Pathway Partitioning. *J. Phys. Chem. A* **2021**, *125*, 6450–6460.

[20] Limão-Vieira, P.; Eden, S.; Mason, N.; Hoffmann, S. Electronic State Spectroscopy of Acetaldehyde, CH3CHO, by High-Resolution VUV Photo-Absorption. *Chem. Phys. Lett.* **2003**, *376*, 737–747.

[21] Smith, A. D.; Warne, E. M.; Bellshaw, D.; Horke, D. A.; Tudorovskya, M.; Springate, E.; Jones, A. J. H.; Cacho, C.; Chapman, R. T.; Kirrander, A.; Minns, R. S. Mapping the Complete Reaction Path of a Complex Photochemical Reaction. *Phys. Rev. Lett.* **2018**, *120*, 183003.

[22] Hockett, P.; Bisgaard, C. Z.; Clarkin, O. J.; Stolow, A. Time-Resolved Imaging of Purely Valence-Electron Dynamics during a Chemical Reaction. *Nat. Physics* **2011**, *7*, 612–615.

[23] Schuurman, M. S.; Blanchet, V. Time-Resolved Photoelectron Spectroscopy: The Continuing Evolution of a Mature Technique. *Phys. Chem. Chem. Phys.* **2022**, *24*, 20012–20024.

[24] Lias, S. G. In *NIST Chemistry WebBook, NIST Standard Reference Database Number 69*; Linstrom, P. J., Mallard, W. G., Eds.; National Institute of Standards and Technology: Gaithersburg , MD, 2022.